Journal of Visualized Experiments

Quantifying the Effects of Antimicrobials on In Vitro Biofilm Architecture Using COMSTAT Software

--Manuscript Draft--

Article Type:	Invited Methods Article - JoVE Produced Video
Manuscript Number:	JoVE61759R1
Full Title:	Quantifying the Effects of Antimicrobials on In Vitro Biofilm Architecture Using COMSTAT Software
Corresponding Author:	Amanda J Morris The Hospital for Sick Children Toronto, Ontario CANADA
Corresponding Author's Institution:	The Hospital for Sick Children
Corresponding Author E-Mail:	amanda.morris@sickkids.ca
Order of Authors:	Amanda J Morris
Additional Information:	
Question	**Response**
Please indicate whether this article will be Standard Access or Open Access.	Standard Access (US$2,400)
Please indicate the **city, state/province, and country** where this article will be **filmed**. Please do not use abbreviations.	Toronto, Ontario, Canada
Please confirm that you have read and agree to the terms and conditions of the author license agreement that applies below:	I agree to the Author License Agreement
Please specify the section of the submitted manuscript.	Immunology and Infection
Please provide any comments to the journal here.	

TITLE:

Quantifying the Effects of Antimicrobials on In vitro Biofilm Architecture Using COMSTAT Software

AUTHORS AND AFFILIATIONS:

Amanda J Morris[1], Alvin Li[1], Lindsay Jackson[1], Yvonne C W Yau[1,2], Valerie Waters[1,3]

[1]Translational Medicine, Hospital for Sick Children, Toronto, ON, CA
[2]Microbiology, Department of Pediatric Laboratory Medicine, Hospital for Sick Children, Toronto, ON, CA
[3]Infectious Diseases, Department of Pediatrics, Hospital for Sick Children, Toronto, ON, CA

Corresponding Author:
Dr. Amanda J Morris
amanda.morris@sickkids.ca

KEYWORDS:

COMSTAT, ImageJ, biofilms, *Pseudomonas aeruginosa*, cystic fibrosis, confocal microscopy, fluorescent staining, antibodies, antibiotics, antimicrobials

SUMMARY:

Antimicrobial-induced changes to *Pseudomonas aeruginosa* biofilm architecture differ among clinical isolates cultured from patients with cystic fibrosis and chronic pulmonary infection. Following confocal microscopy, COMSTAT software can be utilized to quantify variations in biofilm architecture (e.g., surface area, thickness, biomass) for individual isolates to assess the efficacy of anti-infective agents.

ABSTRACT:

Biofilms are aggregates of microorganisms that rely on a self-produced matrix of extracellular polymeric substance for protection and structural integrity. The nosocomial pathogen, *Pseudomonas aeruginosa*, is known to adopt a biofilm mode of growth, causing chronic pulmonary infection in patients with cystic fibrosis (CF). The computer program, COMSTAT, is a useful tool for quantifying antimicrobial-induced changes in *P. aeruginosa* biofilm architecture by extracting data from three-dimensional confocal images. However, standardized operation of the software is less commonly addressed, which is important for optimal reporting of biofilm behavior and cross-center comparison. Thus, the aim of this protocol is to provide a simple and reproducible framework for quantifying in vitro biofilm structures under varying antimicrobial conditions via COMSTAT. The technique is modeled using a CF *P. aeruginosa* isolate, grown in the form of biofilm replicates, and exposed to tobramycin and the anti-Psl monoclonal antibody, Psl0096. The step-by-step approach aims to reduce user ambiguity and minimize the chance of overlooking crucial image-processing steps. Specifically, the protocol emphasizes the elimination of subjective variations associated with the manual operation of COMSTAT, including image segmentation and the selection of appropriate quantitative analysis functions. Although this

method requires users to spend additional time processing confocal images prior to running COMSTAT, it helps minimize misrepresented biofilm heterogenicity in automated outputs.

INTRODUCTION:

Biofilms are aggregates of microorganisms oriented in a matrix of self-produced extracellular polymeric substances (EPS). The EPS matrix is very complex, consisting primarily of bacterial cells, water, proteins, polysaccharides, lipids, and nucleic acids[1], all of which make biofilms distinctly different from free-living planktonic cells. Biofilm EPS are adherent to each other and various surfaces. The EPS matrix has properties that mediate cell-to-cell exchange of metabolites, genetic material, and compounds used for intercellular signaling and defense[2]. These properties collectively provide biofilms structural integrity and protection against external stressors, contributing to immune evasion and antimicrobial resistance[3].

Pseudomonas aeruginosa is a well-recognized nosocomial pathogen, known to adopt an evasive biofilm growth strategy in response to antimicrobials. A prime example of this occurs in patients with the recessive genetic disorder, cystic fibrosis (CF). Biofilms play a pivotal role in the development of antimicrobial-resistant *P. aeruginosa*[4] and permit the establishment of chronic pulmonary infection in patients with CF, causing accelerated decline in lung function and premature mortality[5]. Hence, in vitro biofilm studies are performed to test the efficacy of antibiotics and new anti-infective agents against *P. aeruginosa* isolates obtained from CF patients[6,7]. Following biofilm formation, antimicrobials are applied externally to the structure, and confocal laser scanning microscopy (CLSM) is used to generate high-resolution, three-dimensional reconstructions of biofilm segments. It is common practice to then use the computer software, COMSTAT, to quantify the changes in biofilm architecture[8-11].

Although COMSTAT is a useful tool for quantifying biofilm structure, the reproducibility and standardization of image-processing is less commonly addressed. The image-analysis procedure for example, is objective, but contains an element of subjectivity in the thresholding feature[12,13]. In a similar manner, the COMSTAT program allows the operator to choose from basic to advanced conditions and parameters for image segmentation as well as ten quantitative analysis functions (e.g., thickness distribution, surface area, biomass, dimensionless roughness coefficient). The multitude of user options, compounded with varying operator expertise levels, may result in misguided reporting of biofilm behavior.

Thus, the goal of this protocol is to present a relatively simple method for the quantitative comparison of in vitro biofilm structures using COMSTAT. Herein, three-dimensional images of biofilm segments from a CF *P. aeruginosa* isolate are captured via CLSM using the chambered coverglass model[14]—an established technique used to perform reproducible in vitro biofilm experiments. Utilizing COMSTAT as a plugin to ImageJ, this method allows for researchers to quantitatively identify changes in biofilm architecture in the presence of antimicrobials under varying conditions. Overall, this method aims to eliminate subjective variations associated with the manual operation of COMSTAT, thereby facilitating the standardization of protocols across centers.

PROTOCOL:

1) Bacterial isolate collection

1.1) Obtain *P. aeruginosa* isolates from a cohort of pediatric patients with CF undergoing eradication treatment with inhaled tobramycin at SickKids (Toronto). Freeze isolates at -80 °C in glycerol citrate and sub-culture at least three times prior to use.

2) **In vitro biofilm formation**

NOTE: Use a chambered coverglass method[1] for in vitro biofilm formation with modifications. The overall workflow of this model is shown in **Figure 1**.

2.1) Grow *P. aeruginosa* isolate overnight at 37 °C on blood agar prepared with tryptic soy agar and 5% sheep blood (see **Table of Materials**).

2.2) Inoculate 1–2 bacterial colonies from the blood agar into 4 mL of lysogeny broth (LB). Grow overnight at 37 °C on a shaker set to 225 rpm.

2.3) Prepare a 1:100 dilution of overnight inoculum by adding 40 µL of the culture in 4 mL of fresh LB. Grow for 3–4 h at 37 °C on a shaker set to 225 rpm, to achieve an optical density of approximately 0.1 at 600 nm (OD_{600}) (early log phase).

2.4) Transfer 220 µL of the inoculum to each well of an 8-chambered coverglass slide. Incubate undisturbed at 37 °C for 24 h.

2.5) Slowly remove the medium from each well to prevent the biofilms from detaching at the base.

NOTE: Tilt the slide forward at a 45° angle and aspirate the medium from the bottom corners of each chambered well without touching the base with pipette tip.

2.6) Prepare and slowly add 100 µL of 56 µg/mL fluorescently labelled monoclonal antibody (mAb) (see **Table of Materials**) to the side of the designated chambered wells. Incubate at room temperature (RT) for 1 h to allow antibody attachment to the bacterial antigen epitope.

NOTE: Prior to use, dilute the fluorescently labelled (red) mAb, Psl0096, in LB to obtain a final concentration of 56 µg/mL. Psl0096 is an anti-Psl mAb (optimized affinity derivative of Cam003), which binds to the class I Psl epitope—a key EPS matrix component of *P. aeruginosa* biofilms involved in initial cell attachment and structural integrity[15].

2.7) Prepare and slowly add 100 µL of a 1000 µg/mL antibiotic solution (see **Table of Materials**) to the side of the designated chambered wells. Incubate undisturbed at 37 °C for 24 h.

NOTE: Prior to use, dilute a 50 mg/mL stock of tobramycin antibiotic in LB to obtain a final concentration of 1000 µg/mL.

3) Biofilm fluorescent staining

3.1) Prepare a 0.01 mM solution of a live-cell-staining fluorescent dye. Slowly remove the medium from the chambered wells and add 200 µL of the dye mixture to each well. Incubate at RT in the dark for 45 min.

NOTE: Prior to use, prepare the live cell staining (green) fluorescent dye by adding 4 µL of a 5 mM stock to 2 mL of LB.

3.2) Slowly remove the medium from each well, and wash 2x with 200 µL of fresh LB.

3.3) Add 200 µL of fresh LB to each well and proceed to examination via confocal microscopy.

4) Image acquisition by confocal microscopy

NOTE: The image-processing and COMSTAT analysis procedure is presented in **Figure 2**. Acquire the images of the wells on the same day of biofilm staining. If delay in visualization exceeds 1 h, refrigerate the chambered coverglass in the dark until further processing.

4.1) Acquire images of wells using a confocal microscope system (see **Table of Materials**) with appropriate laser excitation wavelengths and filter sets for acquisition.

NOTE: Here, excite the fluorescently labeled (red) mAb and live cell (green) stain using 561 and 491 nm excitation wavelengths, respectively.

4.2) Capture layered z-stack images (from the substratum to the top of each biofilm segment) in increments of 0.3 µm with a 20–25x water immersion lens. Take a at least 6 image stacks per well.

NOTE: Here, visualize the images using a high-resolution camera with a 25x water immersion lens and processed using image analysis software (see **Table of Materials**). Keep software setup and digital imaging parameters (i.e., brightness and sensitivity) constant for all acquisitions in a single experiment.

4.3) Save images as OME-TIFFs for COMSTAT analysis.

NOTE: Ensure that OME-TIFFs are saved separately for each channel (i.e., red and green). This step varies depending on the image analysis software used.

4.4) Repeat steps 2.1–4.4 to capture images from a total of 3 biological replicates (i.e., 3 independent experiments) per bacterial isolate.

5) COMSTAT Analysis

NOTE: Analyze images quantitatively using the freely available computer program, COMSTAT[16,17], rewritten as a plugin (Comstat2) to ImageJ. Read the general instructions for analyzing image stacks of biofilms within the downloaded package. This contribution provides a summarized protocol, with selected ImageJ processing steps and COMSTAT features recommended for quantifying the effects of antimicrobials on biofilm formation.

5.1) Download the Comstat2 package from http://www.comstat.dk/. Within the installed folder, locate ImageJ and run it.

5.2) Create a source folder on desktop and add a single OME-TIFF to the folder.

5.3) Open OME-TIFF from the source folder, and delete any empty layers containing no biomass. These layers will be either the first or last few layers of the z-stack.

NOTE: Microscope-defined z-stack boundaries are sometimes overestimated by users. Deleting these empty layers establishes a more refined z-stack boundary for COMSTAT analysis.

5.4) Import OME-TIFF in ImageJ by selecting **File | Import | Image Sequence|**. Locate the source folder, highlight without opening it, and click **Select**. A 'Sequence Options' window will appear. Select **OK**.

NOTE: To import additional images in ImageJ, first remove the previous OME-TIFF from the source folder, then add the new OME-TIFF to the folder, and repeat steps 5.3 and 5.4.

5.5) Flip the orientation of the biofilm by selecting **Image | Transform | Flip Z |** to position the substratum as the first (topmost) stack.

NOTE: COMSTAT algorithms read biofilms in the z-direction from top (stack 1) to bottom. It is important to reverse the order of slices by positioning the substratum as image stack 1 to prevent output data from becoming flawed.

5.6) Define image properties by selecting **Image | Properties**. A 'Source' window will appear.

5.6.1) Specify 'Unit of Length' as 'micron'.

5.6.2) Mathematically determine 'Pixel width' and 'Pixel height' using the following equation:

$$\text{Cell size per pixel } (\mu\text{m}) = \frac{\text{physical length of a pixel on CCD}}{\text{total magnification} \times \text{magnifier position}} \quad (1)$$

Here, 'Pixel width' and 'Pixel height' are defined as 0.427, where the physical length of a pixel on the charge-coupled device (CCD) is 16 µm; total magnification is 25x; and magnifier position is 1.5x.

NOTE: The equation used to calculate cell size per pixel may vary depending on the microscope camera manufacturer. Alternately, 'Pixel width' and 'Pixel height' can be defined by spatial calibration (refer to https://imagej.net/Spatial_Calibration).

5.6.3) Define 'Voxel depth' as 0.3 (i.e., incremental space between each z-stack layer). Select **OK** in the 'Source' window.

5.7) Adjust the image threshold by selecting **Image | Adjust | Threshold**. A 'Threshold' window will appear.

NOTE: Objects in the image will appear red with a greyscale background. If threshold is to be adjusted in black and white, use the drop-down menu in the 'Threshold' window to change 'Red' to 'B&W'.

5.7.1) In the image window, adjust the slider to the far right (i.e., topmost layer of the biofilm). To remove background noise, use the 'Threshold' window, which displays a histogram of the image, to manually set the maximum and minimum threshold values. First, set the maximum threshold value by adjusting the lower slider as far right as possible. Second, use the upper slider to adjust the minimum threshold value, which segments the image into two separate phases: red biomass and black background (**Figure 3**).

NOTE: The in vitro biofilm formation and fluorescent microscopy procedure described herein generates OME-TIFFs in the ideal case, allowing for images to be segmented into two distinct phases by means of a simple histogram threshold method. However, in some cases, the histogram distinction between the different phases is not as clear. This can be due to the presence of extensive background noise, varying background intensities, or a low intensity contrast between biomass and background. In such cases, users should adopt an enhanced segmentation procedure[18,19].

5.7.1.1.) Alternatively, adjust thresholds algorithmically for individual images using the left drop-down menu set as 'Default' in the 'Threshold' window. This feature provides 17 different algorithmic threshold options to choose from (refer to https://imagej.net/Auto_Threshold). Select the most applicable option, then 'Auto' to set threshold.

5.7.2) When threshold values are adjusted, use the slider in the image window to scroll through each layer to ensure that background noise is sufficiently removed throughout.

5.7.3) Select **Set** in the 'Threshold' window to first fix the lower threshold value. A 'Set Threshold Levels' window will appear. Select **OK**. Select **Set** again and repeat this step to fix the maximum threshold value.

NOTE: Each time 'Set' is selected, the lower slider may adjust automatically. In such cases, manually re-adjust the slider (or select 'Auto' if using one of the algorithmic thresholds) and repeat steps 5.6.2–5.6.3. The main idea is that whenever the sliders are re-adjusted automatically, 'Set' should be selected an additional two times afterwards to ensure that both the upper and lower thresholds are fixed.

5.7.4) Select **Apply** and a 'Convert Stack to Binary' window will appear. Select **OK**, and then exit the 'Threshold' window.

5.7.5) Save the newly adjusted OME-TIFF by selecting **Plugins | Bio-Formats | Bio-Formats Exporter|**. Enter a new file name and save as OME-TIFF in the source folder. A 'Bio-Formats Exporter – Multiple Files' window will appear. Select **OK**. A 'Bio-Formats Exporter Options' window will appear. Select **OK**.

NOTE: Ensure that only the newly adjusted, Black and White OME-TIFF(s) are saved in the source folder before proceeding to COMSTAT analysis. Remove all original OME-TIFFs from the folder.

5.8) Run COMSTAT by selecting **Plugins | Comstat2 |**. An 'About' window will appear. Select **OK**. Three windows will appear.

5.8.1) In the 'Observed Directories' window (top right), select **Add**. Locate the source folder, highlight without opening it, and click **Choose**. An 'Images in Directories' window will appear (top left) that lists the OME-TIFFs to be analyzed via COMSTAT.

5.8.2) On the 'Comstat 2.1' window (bottom right), de-select 'Automatic thresholding (Otsu's method)' to ensure that the software uses threshold values previously set up for individual OME-TIFFs. Also, de-select **Connected Volume Filtering** (CVF) to ensure that very thin parts of the biofilm as well as free floating cells or biomass found within voids of the biofilm structure are included in the analysis.

NOTE: Here, de-select CVF because COMSTAT analysis is performed on very early biofilms (24 h initial growth) and remaining planktonic cells/colonies post antimicrobial treatment. For mature biofilms, select CVF to ensure that only biomass connected to the biofilm structure is quantified.

5.8.3) On the 'Comstat 2.1' window (bottom right), select desired features for quantitative analysis. Here, select **Bio Mass, Thickness Distribution,** and **Surface Area**. Select **Go** to run the program. In the 'Log' window (bottom left), the output data are shown processing until 'Done with selected functions/images!' appears. Record the COMSTAT measurements. These measurements are also automatically saved as TXT files in the source folder.

REPRESENTATIVE RESULTS:

A *P. aeruginosa* isolate cultured from an infected CF patient is used to demonstrate the strengths of this approach in accurately quantifying antimicrobial-induced changes in in vitro biofilm architecture. The overall workflow of this model is represented in **Figure 1**. The image-processing

and COMSTAT analysis procedure is shown in **Figure 2**. A simple histogram thresholding approach for image segmentation, applied to an CLSM OME-TIFF, is shown in **Figure 3**. Biofilm structural changes caused by tobramycin and anti-Psl mAb, Psl0096, is shown in **Figure 4**. Representative confocal images of biofilm segments separated into live cell (green) and antibody (red) channels are shown in **Figure 4A**. Corresponding data of three COMSTAT parameters, including average biofilm thickness, biomass, and surface-to-biovolume ratio are shown in **Figure 4B-D**. Overall, COMSTAT data demonstrate significant differences among biofilm structures compared to control wells. With tobramycin, a clear reduction in average thickness and biomass can be observed in **Figure 4B** and **Figure 4C**, respectively. However, in the presence of the anti-Psl mAb, Psl0096, the *P. aeruginosa* biofilm is resistant to tobramycin. When examining surface-to-biovolume ratio (**Figure 4D**), a significant reduction is observed with anti-Psl mAb, Psl0096 ($p < 0.0001$), in both tobramycin-exposed and unexposed biofilms, representing the formation of aggregates (**Figure 4A**).

FIGURES AND TABLES:

Figure 1: In vitro biofilm formation. A *Pseudomonas aeruginosa* isolate is grown on blood agar and inoculated in LB overnight. The overnight culture is diluted 1:100 and grown to early log phase (3–4 h incubation) to obtain a final OD_{600} of approximately 0.1. The OD-adjusted inoculum is seeded into each well of an 8-chambered coverglass and grown for 24 h, allowing biofilms to attach and mature at the base of the wells. Media is carefully removed from the wells, and a fluorescent labelled (red) mAb is added to the designated wells. The chambered coverglass is incubated for 1 h, allowing the antibody to bind to the bacterial antigen epitope. The antibiotic is added to designated wells, and biofilms are grown for 24 h. Medium is removed from the wells, and a live-cell fluorescent (green) stain is added. Following 45 min of incubation, the wells are washed 2x with fresh LB, and confocal imaging is performed in LB.

Figure 2: Image-processing and COMSTAT analysis. Comstat2, as a plugin to ImageJ, is used for the quantitative analysis of in vitro biofilm architecture. (**A**) Initial setup is performed by first opening the ImageJ program found within the downloaded Comstat2 package. It is then recommended to create a source folder, from which a single OME-TIFF can be added and imported into ImageJ. Once imported, the OME-TIFF is deleted from the source folder. * These steps can be repeated to add additional OME-TIFFs, allowing the operator to process multiple images at a time. (**B**) Image-processing is performed entirely in ImageJ. The orientation of OME-TIFF is flipped in the z-direction, assigning the first layer of biofilm substratum as stack 1. ** This step is only necessary if the OME-TIFF output from the confocal microscope is inverted. Image properties are defined, and the threshold of OME-TIFF is adjusted manually. The Bio-formats Exporter plugin is used to save the newly adjusted OME-TIFF in source folder. (**C**) COMSTAT analysis is performed using the Comstat2 plugin. The source folder containing the OME-TIFF(s) is added. Specific features that may flaw results are de-selected, while desired features for quantitative analysis are selected. 'Run' is selected to initiate analysis. Once completed, measurements are recoded from TXT files automatically saved in the source folder.

Figure 3. Simple Histogram Thresholding of a 16-bit CLSM OME-TIFF in ImageJ. (**A**) OME-TIFF before thresholding with background noise and two distinct phases: red biomass and black

background. (**B**) Threshold window used to remove background noise and set optimal threshold by converting lower intensity pixels (values less than the minimum set threshold) into black background. Maximum threshold value set to establish gray level range to be converted to biomass (red). (**C**) Generated quality segmented image. (**D**) Converted stack to a binary black and white image that is readable to COMSTAT algorithms.

Figure 4. Representative CLSM images and COMSTAT comparison of fluorescently labelled CF *Pseudomonas aeruginosa* biofilms under varying antimicrobial conditions. (**A**) Three-dimensional images of 48 h biofilms grown in chambered coverglass. Live-cell (green) channel of biofilm grown in LB media alone (top left) and with 1000 µg/mL tobramycin (bottom left), representing antibiotic effect on control wells. Live-cell channel of biofilm exposed to anti-Psl mAb, Psl0096, in the absence (top middle) and presence (bottom middle) of tobramycin, showing the formation of aggregates and tobramycin resistance. Corresponding Psl0096 (red) channel of identical biofilm is shown in the absence (top right) and presence (bottom right) of tobramycin. White arrows indicate high Psl-antibody binding localized in the same region of aggregates shown in the live cell channel. Quantitative comparison of COMSTAT parameters are displayed in a series of bar graphs, including (**B**) average thickness (entire well), (**C**) biomass, and (**D**) surface-to-biovolume ratio of the isolate. One scale unit is equivalent to 19.68 µm. Each bar represents average of multiple images (n=18) from 3 biologically independent experiments, in the absence (grey bars) and presence (black bars) of tobramycin, with standard error bars of the mean. *p <0.01 **p <0.001 ***p < 0.0001 by Mann-Whitney test.

DISCUSSION:

There is no prescribed method for quantitatively comparing three-dimensional images of in vitro biofilm structures, and procedures described in this context are often difficult to standardize due to inter-operator variability[20]. Thus, this protocol offers a simple and reproducible framework for COMSTAT applications seeking to quantify changes in in vitro biofilm architecture under varying antimicrobial conditions. The strengths of this technique are modeled using a CF *P. aeruginosa* isolate, grown in the form of biofilm replicates, and exposed to tobramycin and the anti-Psl mAb, Psl0096.

One of the most critical steps outlined in this protocol, as well as in related work, is image thresholding[13,21]. The image thresholding procedure is a segmentation technique, which reduces greyscale images into a readable black-and-white format for COMSTAT algorithms. During this process, it is important to effectively differentiate which greyscale pixels should be considered biomass (black) versus background noise (white), otherwise the threshold value will change the volume and morphology assigned to an individual biofilm image[22]. Thresholding can be performed in many different ways in ImageJ: manually or algorithmically by one of 17 options; set for individual images or by applying a fixed value (determined by the user) to a group of images[17]; applied to the entire image (global); or algorithmically applied to specific regions (local)[23,24] of an 8-bit image. The chosen method for thresholding and how it is performed is up to the discretion of the operator, which can introduce significant errors in biofilm image analysis and lead to vastly different results.

In the present protocol, global thresholding was performed manually to segment individual 16-bit images. Although algorithmic methods have advantages over manual, including elimination of user intervention[13,22] and reduced time spent on image-processing (especially for large data sets)[25], they do not account for the wide characteristic variability of images from heterogenous samples, as observed among *P. aeruginosa* isolates[26-28]. Previous work suggests that to numerically correlate biofilm activity with architectural changes, it is necessary to threshold images in a way that emulate biofilm heterogeneity [29,30]. Available algorithms in ImageJ for thresholding are considered less suitable given their inconsistencies with expert-determined values[30], and technological limitations, including an inability to segment discrete geometric properties[22]. These algorithms are also limited because very few studies have evaluated their strengths and weaknesses with respect to manual operations. Without a consensus on the best algorithm for thresholding, manual eye-based methods in ImageJ remain most suitable[13,17].

Apart from thresholding, CVF is another segmentation process that can be used to remove additional background noise from three-dimensional biofilm images (e.g., planktonic elements that are not attached to the biofilm structure). However, when analyzing early biofilms, utilizing CVF runs the risk of generating null or unexpectedly low COMSTAT outputs because the function assumes that all biofilms grow in a connected fashion from the substratum[31]. A biofilm may consist of spatial structures, such as voids or channels filled with fluids and floating cells[32,33], which CVF inaccurately excludes from the analysis. In the study described herein, de-selection of CVF is important, especially because COMSTAT is performed to quantify the remaining planktonic cells/colonies post antimicrobial treatment. Similarly, under certain conditions, different bacterial strains produce very thin areas within the biofilm that are undetected by the CVF feature due to the set voxel depth[16] (in this case, 0.3 µm), and are subsequently removed from the analysis. Therefore, the present study de-selects CVF to prevent null outputs or undercalculations of biomass.

A final critical step of the protocol involves selecting quantitative analysis functions that best represent morphological changes to biofilm architecture. Here, biomass, thickness distribution, and surface area are assessed. COMSTAT parameters that quantify biomass and thickness are widely used in studies that describe structural changes to *P. aeruginosa* biofilms[8-11,14,27]. Although less frequently interpreted, surface-to-biovolume ratio (among the surface area outputs) is found herein to be most effective in quantifying aggregation—an important mechanism of antimicrobial resistance, preventing anti-infective agents from penetrating the full depth of biofilms[5]. This observation is consistent with previous work, which determined a negative correlation of surface-to-biovolume ratio to be indicative of densely clustered bacterial cells[34,35]. Furthermore, a closely related study reported a 2.6-fold higher surface-to-biovolume ratio among flat formed, undifferentiated PA01 biofilms compared to an overproducing-Psl strain, which visually formed aggregates described as hyper-biofilm structures[36]. Notably, because of the inherent complexity of biofilms, it is typical to generate variable COMSTAT results, regardless of chosen analysis function and even if experimental conditions are kept constant. Therefore, all quantitative measurements of CLSM images should be performed with a minimum of 3 biological replicates and a consistent number of z-stack images per condition, accompanied by statistical analysis.

Overall, a key approach in quantifying CLSM images via COMSTAT is in the development of a standardized framework for software operation and analysis. To our knowledge, such an integration does not exist, but rather there is a surplus of biofilm cultivation frameworks, image segmentation techniques, and operational parameters applied to different studies. In the absence of a gold standard, this protocol offers an important step toward transparency across laboratories involved in determining the effects of antimicrobials against in vitro biofilm formation. A limitation of this technique is that it does not include a dual fluorescent staining procedure to differentiate live cells from dead cells. Thus, future applications of this method may wish to incorporate a viability assay, as an internal control to determine viable cell numbers. Likewise, a crystal violet assay may be used to correlate relative cell density with microscopy results. With the rise of new mathematical modeling and algorithmic plugins for image segmentation, it may also be worth investigating different ways to refine this protocol to better depict the heterogenicity of biofilms. This may include scripts for capturing the irregularities of biofilm matrices, spatial coherence of segmented voxels and channels, and localized thresholds. In terms of clinical application, this protocol may be useful for measuring the therapeutic success of different antimicrobials used to treat biofilm infections. It may also be valuable for testing various strategies used to disrupt biofilms to make them more susceptible to antimicrobial treatment.

ACKNOWLEDGMENTS:

The authors would like to acknowledge Cystic Fibrosis Foundation for providing funding for this research.

DISCLOSURES:

None

REFERENCES:

1. Flemming, H.C., Wingender, J. The biofilm matrix. *Nature Reviews Microbiology.* **8**, 623–633 (2010).
2. Flemming, H. C. et al. Biofilms: an emergent form of bacterial life. *Nature Reviews Microbiology.* **14**, 563-575 (2016).
3. Rybtke, M., Hultqvist, L. D., Givskov, M., Tolker-Nielsen, T. *Pseudomonas aeruginosa* biofilm infections: community structure, antimicrobial tolerance and immune response. *Journal of Molecular Biology.* **427**, 3628-3645 (2015).
4. Wendel, A. F., Ressina, S., Kolbe-Busch, S., Pfeffer, K., MacKenzie, C. R. Species diversity of environmental GIM-1-producing bacteria collected during a long-term outbreak. *Applied and Environmental Microbiology.* **82**, 3605-3610 (2016)
5. Costerton, J. W., Stewart, P. S., Greenberg, E. P. Bacterial biofilms: a common cause of persistent infections. *Science.* **284**, 1318-1322 (1999).
6. Powell, L. C. et al. Targeted disruption of the extracellular polymeric network of *Pseudomonas aeruginosa* biofilms by alginate oligosaccharides. *NPJ Biofilms and Microbiomes.* **4**, 1-10 (2018).

7. Ciofu, O., Tolker-Nielsen, T., Jensen, P.Ø., Wang, H., Høiby, N. Antimicrobial resistance, respiratory tract infections and role of biofilms in lung infections in cystic fibrosis patients. *Advanced Drug Delivery Reviews.* **85**, 7-23 (2015).
8. Landry, R. M., An, D., Hupp, J. T., Singh, P. K., Parsek, M. R. Mucin–*Pseudomonas aeruginosa* interactions promote biofilm formation and antibiotic resistance. *Molecular Microbiology.* **59**, 142-151 (2006).
9. Beaudoin, T. et al. *Staphylococcus aureus* interaction with *Pseudomonas aeruginosa* biofilm enhances tobramycin resistance. *NPJ Biofilms and Microbiomes.* **3**, 1-9 (2017).
10. Rojo-Molinero, E. et al. Sequential treatment of biofilms with aztreonam and tobramycin is a novel strategy for combating *Pseudomonas aeruginosa* chronic respiratory infections. *Antimicrobial Agents and Chemotherapy.* **60**, 2912-2922 (2016).
11. Hentzer, M. et al. Alginate overproduction affects *Pseudomonas aeruginosa* biofilm structure and function. *Journal of Bacteriology.* **183**, 5395-5401 (2001).
12. Tolker-Nielsen, T., Sternberg, C. Growing and analyzing biofilms in flow chambers. *Current Protocols in Microbiology.* **21**, 1-17 (2011).
13. Luo, T. L. et al. A Sensitive thresholding method for confocal laser scanning microscope image stacks of microbial biofilms. *Scientific Reports.* **8**, 1-14 (2018).
14. Beaudoin, T., Kennedy, S., Yau, Y., Waters, V. Visualizing the effects of sputum on biofilm development using a chambered coverglass model. *Journal of Visualized Experiments.* **118**, e54819 (2016).
15. DiGiandomenico, A. et al. Identification of broadly protective human antibodies to *Pseudomonas aeruginosa* exopolysaccharide Psl by phenotypic screening. *Journal of Experimental Medicine.* **209**, 1273-1287 (2012).
16. Heydorn, A. et al. Quantification of biofilm structures by the novel computer program COMSTAT. *Microbiology* **146**, 2395-2407 (2000).
17. Vorregaard, M. Comstat2 - a modern 3D image analysis environment for biofilms, in Informatics and Mathematical Modelling. Technical University of Denmark: Kongens Lyngby. Denmark (2008).
18. Hashemi, M. A., Khaddour, G., François, B., Massart, T. J., Salager, S. A tomographic imagery segmentation methodology for three-phase geomaterials based on simultaneous region growing. *Acta Geotechnica.* ***9***, 831-846 (2014).
19. Rogowska, J. Overview and fundamentals of medical image segmentation. *Handbook of Medical Image Processing and Analysis.*73-90 (2009).
20. Webb, D. et al. Assessing technician effects when extracting quantities from microscope images. *Journal of Microbiological Methods.* **53**, 97-106 (2003).
21. Azeredo, J. et al. Critical review on biofilm methods. *Critical Reviews in Microbiology* **43**, 313-351 (2017).
22. Xavier, J. B. et al. Objective threshold selection procedure (OTS) for segmentation of scanning laser confocal microscope images. *Journal of Microbiological Methods.* **47**, 169-180 (2001).
23. Arena, E. T. et al. Quantitating the cell: turning images into numbers with ImageJ. *Wiley Interdisciplinary Reviews: Developmental Biology.* **6**, e260 (2017).

24. Daims, H., Wagner, M. Quantification of uncultured microorganisms by fluorescence microscopy and digital image analysis. *Applied Microbiology and Biotechnology.* **75**, 237-248 (2007).
25. Yerly, J., Hu, Y., Jones, S. M., Martinuzzi, R. J. A two-step procedure for automatic and accurate segmentation of volumetric CLSM biofilm images. *Journal of Microbiological Methods.* **70**, 424-433 (2007).
26. Lee, B. et al. Heterogeneity of biofilms formed by nonmucoid *Pseudomonas aeruginosa* isolates from patients with cystic fibrosis. *Journal of Clinical Microbiology.* **43**, 5247-5255 (2005).
27. Stapper, A. P. et al. Alginate production affects *Pseudomonas aeruginosa* biofilm development and architecture, but is not essential for biofilm formation. *Journal of Medical Microbiology.* **53**, 679-690 (2004).
28. Reichhardt, C., Parsek, M. Confocal laser scanning microscopy for analysis of *Pseudomonas aeruginosa* biofilm architecture and matrix localization. *Frontiers in Microbiology.* **10**, 677 (2019).
29. Yang, X., Beyenal, H., Harkin, G., Lewandowski, Z. Quantifying biofilm structure using image analysis. *Journal of Microbiological Methods.* **39**, 109-119 (2000).
30. Yang, X., Beyenal, H., Harkin, G., Lewandowski, Z. Evaluation of biofilm image thresholding methods. *Water Research.* **35**, 1149-1158 (2001).
31. Ross, S. S. et al. Quantification of confocal images of biofilms grown on irregular surfaces. *Journal of Microbiological Methods.* **100**, 111-120 (2014).
32. Ma, L. et al. Assembly and development of the *Pseudomonas aeruginosa* biofilm matrix. *PLoS Pathogens.* **5** (2009).
33. Mah, T. F. et al. A genetic basis for *Pseudomonas aeruginosa* biofilm antibiotic resistance. *Nature.* **426**, 306-310 (2003).
34. Srinandan, C. S., Jadav, V., Cecilia, D., Nerurkar, A. S. Nutrients determine the spatial architecture of *Paracoccus sp.* biofilm. *Biofouling.* **26**, 449-459 (2010).
35. Ramos, I., Dietrich, L. E., Price-Whelan, A., Newman, D. K. Phenazines affect biofilm formation by *Pseudomonas aeruginosa* in similar ways at various scales. *Research in Microbiology.* **161**, 187-191 (2010).
36. Ma, L., Jackson, K. D., Landry, R. M., Parsek, M. R., Wozniak, D. J. Analysis of *Pseudomonas aeruginosa* conditional psl variants reveals roles for the psl polysaccharide in adhesion and maintaining biofilm structure postattachment. *Journal of Bacteriology.* **188**, 8213-8221 (2006).

Figure 1

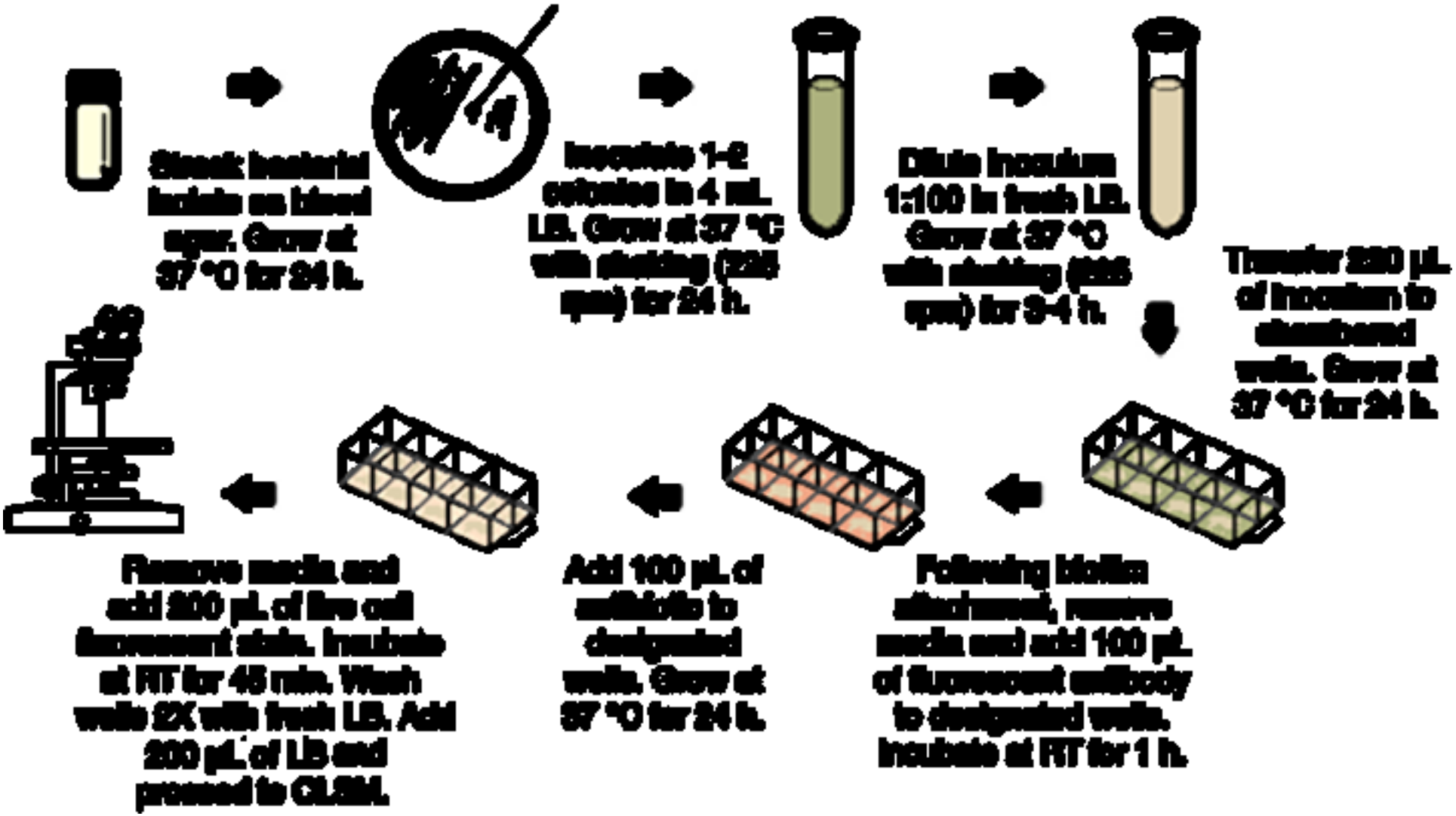

Figure 2

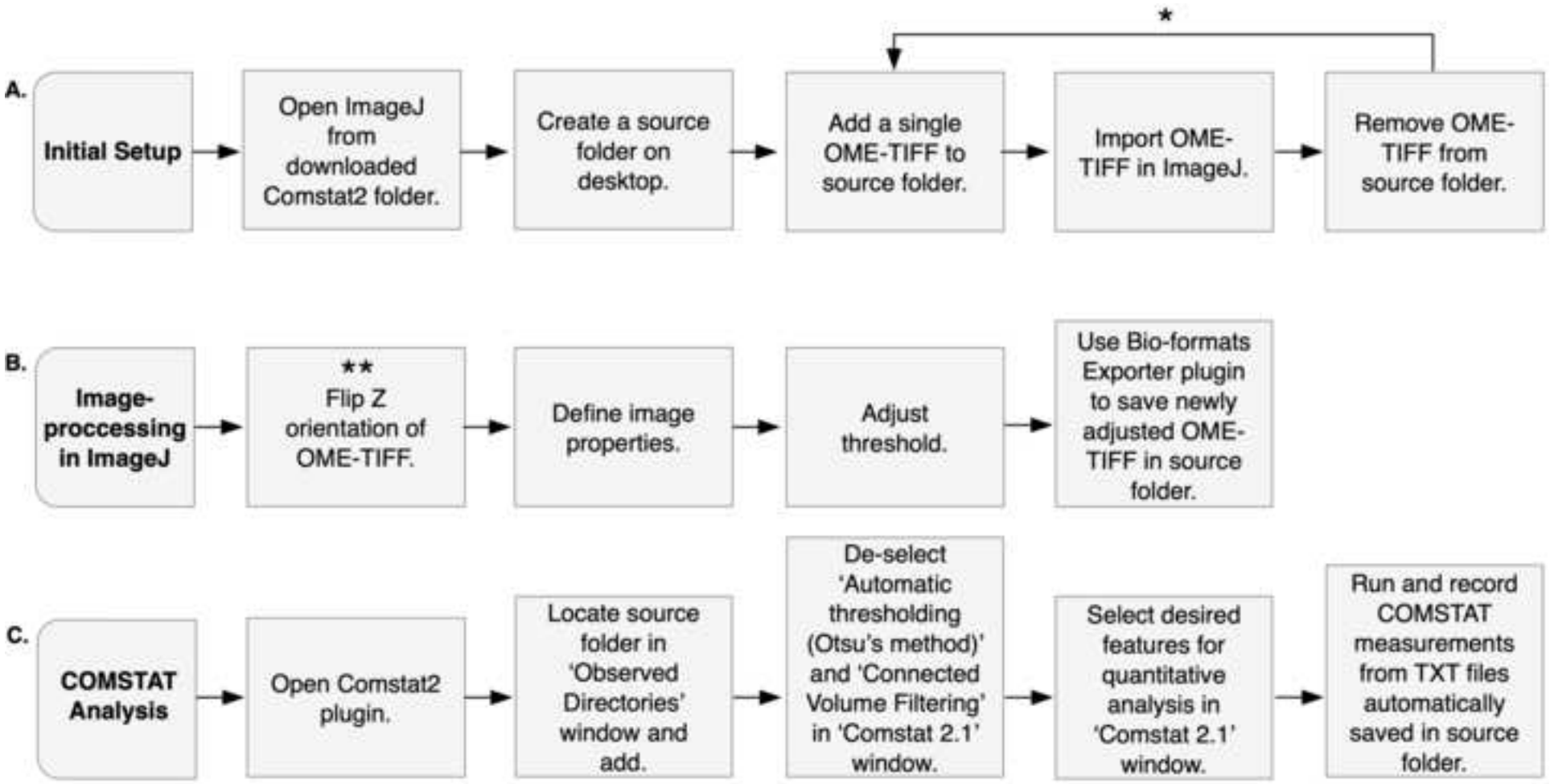

Figure 3

Click here to access/download;Figure;Picture3.tif

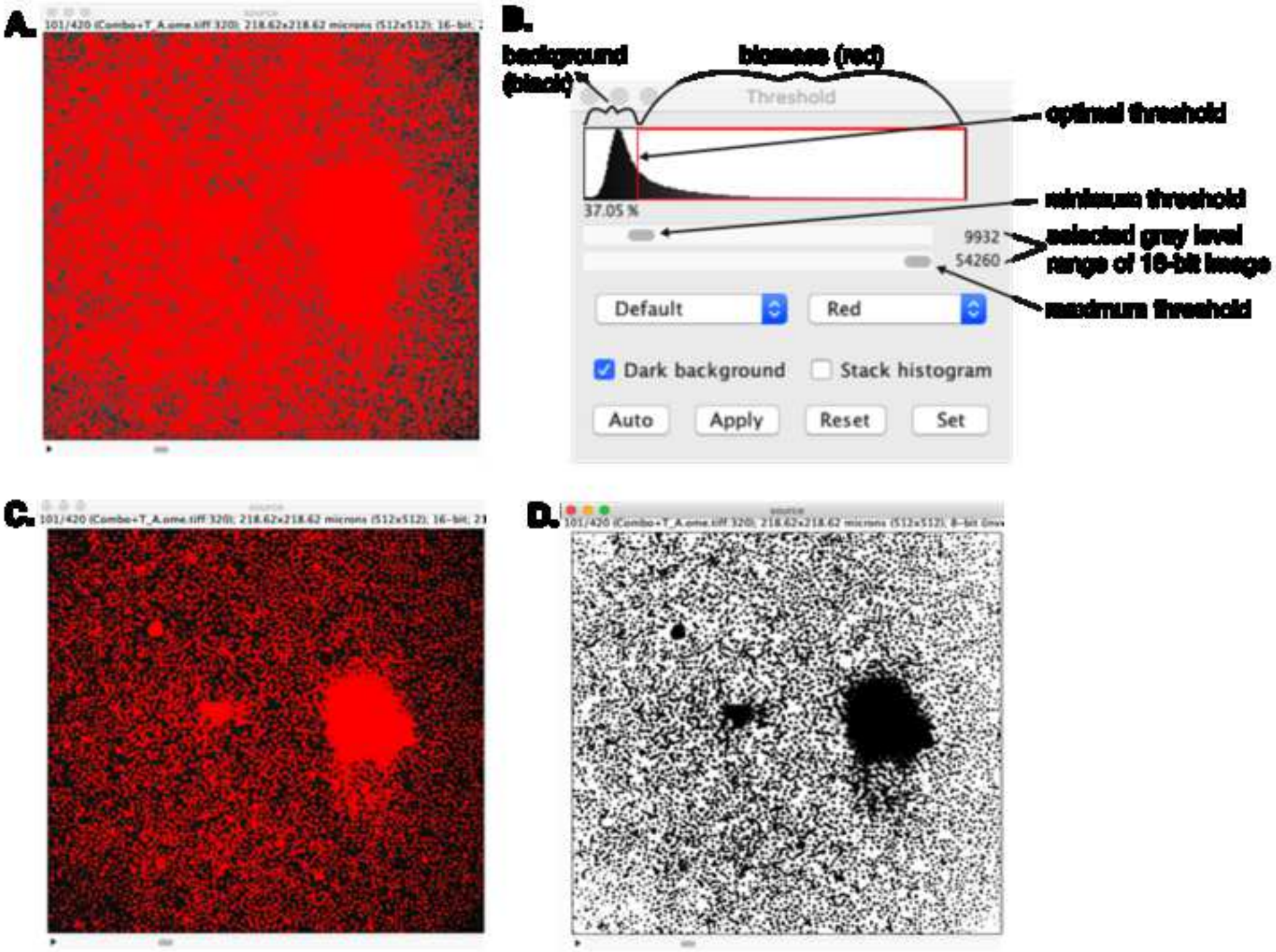

Figure 4

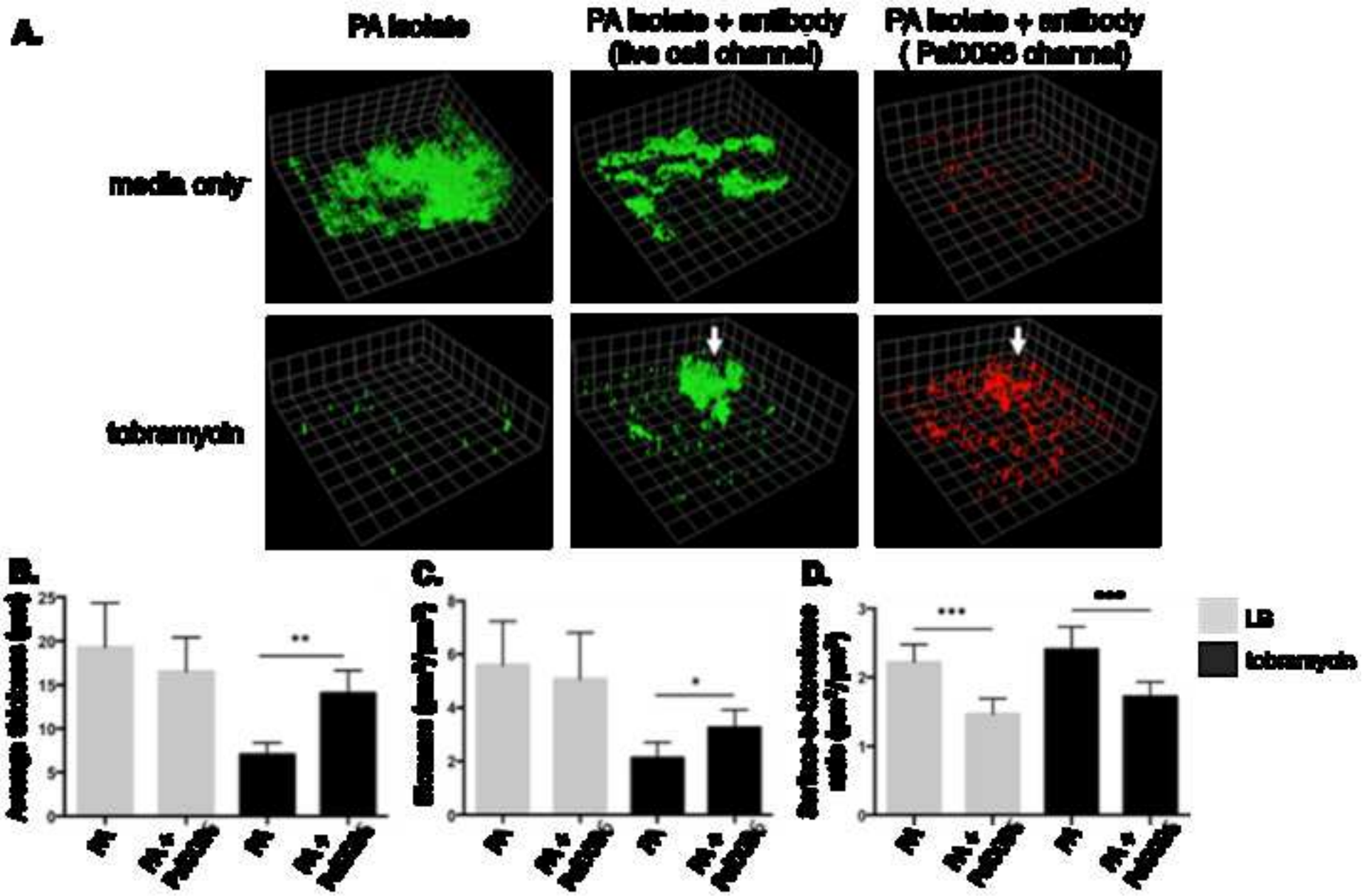

Table

Name of Material/Equipment	Company	Catalog Number
Anti-Psl mAb, Psl0096	Medimmune	
Blood Agar (TSA with 5 % Sheep Blood) Medium	Fisher Scientific	R01200
Eight-well Chambered Coverglass w/ non-removable wells	Thermo Fisher Scientific	155411
Invitrogen SYTO 9 Green Fluorescent Nucleic Acid Stain	Thermo Fisher Scientific	S34854
LB BROTH (LENNOX), Liquid	BioShop Canada	LBL666
Tobramycin, 900 µg/mg	Alfa Aesar by Thermo Fisher Scientifi	J66040
Quorum Volocity 6.3	Quorum Technologies	

Comments/Description
It is recommended to perform a minimal inhibitory concentration (MIC) test for every batch made to ensure quality control of antimicrobial p
Image analysis software

ɔotency

Manuscript JoVE61759
Response to Reviewers

Dear Dr. Nguyen,

Thank you for giving us the opportunity to revise our manuscript "Quantifying the Effects of Antimicrobials on *In Vitro* Biofilm Architecture using COMSTAT Software" for publication in the *Journal of Visualized Experiments*. We appreciate the time and effort you and the reviewers have put forth in providing insightful feedback on our manuscript. We have revised our manuscript to address reviewers' suggestions.

Please see below, in boxes, line-by-line responses to the reviewers' comments and concerns. All corresponding page numbers refer to the revised copy of our manuscript.

Sincerely,

Amanda Morris, Ph.D.

Reviewer 1

Comment stating that the manuscript is well organized and written with a clear description of some specific protocols.

Authors' response:

Thank you!

Major comment indicating that the paper does not present any new information, which researchers are not already doing.

Authors' response:

Thank you for your comment. While we do recognize that this paper does not offer *new* information about COMSTAT, it does synthesize the extensive amount of information available in literature for operating the software into a user-friendly and logical guide.

Major comment indicating that the manuscript lacks complete information about the nature of mature biofilms.

Authors' response:

Thank you for your comment. Typically, 24 h biofilm growth is performed in studies that aim to investigate the effects of antimicrobials on pseudomonas biofilm formation (e.g., References 7, 9, 14, 33, 35). The first 24 h lays down the foundation of biofilm growth and the addition of antimicrobial(s) in the subsequent 24 h examines how it affects the biofilm architecture. We wanted to keep our protocol consistent with these studies.

Major comment indicating that our protocol does not include a wash step after inoculation, before treatment or after treatment, which makes it in unclear whether cell debris or planktonic cells interfere with biofilm quantification. This issue is seen further as we instruct users to de-selects connected volume filtering (CVF), which can create many confusions to different researchers and may produce misinterpretations in biofilm quantification.

Authors' response:

Thank you for your comment. Given that we are working with very early biofilms, having multiple wash steps would run the risk of disrupting the biofilm/cells laid down after 24 h. In addition, throughout the protocol we are continuously aspirating and adding media. For example, after the initial inoculation, we remove the growth media prior to adding the antibiotic; thus, even though we did not wash (to prevent biofilm disruption), we would have removed planktonic cells from the wells. Also, after fluorescent staining, we wash 2X with fresh LB (line 139 and lines 314-315). The number of wash steps included in our protocol is consistent with previous work (References 9, 14).

For clarification, we have added the following text:

Lines 275-278: NOTE: Here, CVF is de-selected because COMSTAT analysis is performed on very early biofilms (24 h initial growth) and remaining planktonic cells/colonies post antimicrobial treatment. For mature biofilms, CVF should remain selected to ensure that only biomass connected to the biofilm structure is quantified.

Lines 396-399: However, when analyzing early biofilms, utilizing CVF runs the risk of generating null or unexpectedly low COMSTAT outputs because the function assumes all biofilms grow in a connected fashion from the substratum[31].

Lines 400-402:	In the study described herein, de-selection of CVF is important, especially since COMSTAT is performed to quantify the remaining planktonic cells/colonies post antimicrobial treatment.

Major comment suggesting that the image acquisition and confocal microscopy steps (lines 151-155) is specific to authors' system and should be generalized or at least specified that each researcher/laboratory uses different software and microscopes.

Authors' response:

Thank you for bringing this to our attention. We have generalized the statement by removing details specific to our image acquisition and confocal microscope system. The revised text reads as follows:

Lines 161-162:	NOTE: Ensure to save OME-TIFFs separately for each channel (*i.e.*, red and green). This step varies depending on the image analysis software used.

Major comment regarding why we eliminate white/empty layers (lines 222 and 224) from the OME-TIFF. Also, mentioning that is we keep CVF selected, this step is not important.

Authors' response:

Thank you for your comment. When establishing the z-stack boundaries using the microscope fine adjustment (Step 4.2 – lines 152-154), we noticed that sometimes human error leads to overestimated boundaries. This is especially noticeable when you open up the OME-TIFFs and see individual empty layers (either the first or last few layers of the z-stack). We agree that if CVF is selected this step is not necessary. However, when CVF is de-selected, this step is crucial because it affects COMSTAT outputs (particularly, the surface-to-biovolume ratio parameter).

In the revised manuscript, we have removed step 5.6.6 entirely. However, reinstated the step, along with a note, at an earlier stage of the protocol. The revised text reads as follows:

Lines 179-183:	Open OME-TIFF from source folder and delete any empty layers containing no biomass. These layers will be either the first or last few layers of the z-stack. NOTE: Microscope-defined z-stack boundaries are sometimes overestimated by users. Deleting these empty layers establishes a more

refined z-stack boundary for COMSTAT analysis.

Major comment indicating that references need to be reformatted, especially the name of bacteria which should be in cursive.

Authors' responses:

Thank you for bringing this to our attention. We have reformatted our references to follow JoVE guidelines. All names of bacteria (*i.e., Pseudomonas aeruginosa*, *Staphylococcus aureus* and *Paracoccus sp.*) have been italicized.

Reviewer 2

Minor concern indicating that the names of bacteria in references must be written in italics.

Authors' response:

Thank you for bringing this to our attention. All names of bacteria (*i.e., Pseudomonas aeruginosa*, *Staphylococcus aureus* and *Paracoccus sp.*) have been italicized in reference list.

Reviewer 3

Major concern indicating that our manuscript does not provide evidence in literature to suggest that inconsistencies and/or differences in analyzing biofilms via COMSTAT leads to conflicting results. Also, there is no evidence presented to suggest that using different methods may result in different conclusions.

Authors' response:

Thank you for bringing this to our attention. This is a very valid point. Internally, we observed inconsistencies in COMSTAT outputs depending on how the operator used the software (*e.g.,* whether they included or excluded certain steps outlined in our protocol). However, we recognize that such evidence is not presented; thus, all statements suggesting "inconsistencies in results describing biofilm behaviour" have been revised as follows:

Lines 34-36: However, standardized operation of the software is less commonly addressed, which is important for optimal reporting of biofilm behaviour and cross-centre comparison.

Lines 76-77: The multitude of user options, compounded with varying operator expertise levels, may result in misguided reporting of biofilm behaviour.

Comment stating that our manuscript would be more impactful if different approaches to image analysis were compared to our approach to see whether they change conclusions.

Authors' response:

Thank you for your comment. This would be interesting to investigate further in future studies.

Reviewer 4

Major concern regarding step 5.6.1) (line 197). Criteria for setting threshold values should be more clearly specified.

Authors' response:

Thank you for your comment. This is a very valid point. Image thresholding is arguably the most critical step in image processing that warrants further specification in our protocol. We have revised step 5.6.1) to following:

Lines 221-238 On the image window, adjust slider to the far right (*i.e.*, topmost layer of the biofilm). To remove background noise, use the 'Threshold' window, which displays a histogram of the image, to manually set the maximum and minimum threshold values. First, set the maximum threshold value by adjusting the lower slider as far right as possible. Second, use the upper slider to adjust the minimum threshold value, which segments the image into two separate phases: red biomass and black background (Figure 3).
NOTE: The *in vitro* biofilm formation and fluorescent microscopy procedure described herein generates OME-TIFFs in the ideal case, allowing for images to be segmented into two distinct phases by means of a simple histogram threshold method. However, in some cases, the histogram distinction between the different phases is not as clear. This can be due to the presence of extensive background noise, varying background intensities, or a low intensity contrast between biomass and

background. In such cases, users should adopt an enhanced segmentation procedure[18,19].

In addition, we have added Figure 3 (line 622) and corresponding figure legend (lines 333-339).

Minor concern regarding lines 225-227. Problems encountered when removing the original OME-TIFF prior to running COMSTAT on the exported file.

Authors' response:

Thank you for testing our protocol and pointing out the error you encountered. We recognize that the error is due to step 5.6.6) (lines 222-224), which instructs users to "Further adjust OME-TIFF by opening the file from source folder and deleting any white (empty) layers containing no biomass. These layers will be either the first or last few layers of the z-stack". We realized that if users further adjust the final black and white OME-TIFF (*i.e.,* following Bio-Format Exporters), than COMSTAT is unable to read the file. Therefore, any deletion of empty layers must be done to the original greyscale OME-TIFF, so that users do not encounter this error. We have removed step 5.6.6.) and added the following as step 5.3):

Lines 179-183: Open OME-TIFF from source folder and delete any empty layers containing no biomass. These layers will be either the first or last few layers of the z-stack.
NOTE: Microscope-defined z-stack boundaries are sometimes overestimated by users. Deleting these empty layers establishes a more refined z-stack boundary for COMSTAT analysis.

Reviewer 5

Comment stating that this manuscript offers an overall straightforward guide to setting up samples and analyzing microscopy images.

Authors' response:

Thank you! Our motivation for writing the paper was to provide a user-friendly guide that offers readers straightforward steps.

Note suggesting that the use of a wet bench method could help to correlate and confirm microscopy results.

Authors' response:

Thank you for your comment. Yes, we agree. In our lab we typically correlate and confirm our microscopy results using a viability assay, which measures the luminescence of metabolically active cells (*i.e.*, ATP present). In this particular paper, we decided to not include these steps as we thought they would stray away from the core focus of our paper, which is COMSTAT quantification. However, we did mention in the discussion (lines 433-435) that "future applications of this method may wish to incorporate a viability assay, as an internal control to determine viable cell numbers". We have since added to this statement by also suggesting that a crystal violet assay could be utilized. The revised statement reads as follows:

Lines 433-436	Thus, future applications of this method may wish to incorporate a viability assay, as an internal control to determine viable cell numbers. Likewise, a crystal violet assay may be used to correlate relative cell density with microscopy results.

Minor concern noting that step 4.1) (lines 135-136) can be written as a note rather than a standalone step.

Authors' response:

Thank you for bringing this to our attention. We have since changed step 4.1) to the following note:

Line 144-145	NOTE: Wells are imaged the same day of biofilm staining. If delay in visualization exceeds 1 h, chambered coverglass is kept refrigerated in dark until further processing.

Minor concern indicating that Figure 3. bar graph is missing a legend.

Authors' response

Figure 3 (Figure 4 in revised copy) has been modified to include a bar graph legend.